

Original Article

Effects of neferine on Kv4.3 channels expressed in HEK293 cells and ex vivo electrophysiology of rabbit hearts

Chen WANG^{1, #}, Yu-fang CHEN^{1, #}, Xiao-qing QUAN², Huan WANG¹, Rui ZHANG¹, Jun-hua XIAO¹, Jia-ling WANG¹, Cun-tai ZHANG², Ji-zhou XIANG¹, Qiang TANG^{1, *}

¹Department of Pharmacology, School of Basic Medicine, Tongji Medical College, Huazhong University of Science and Technology, Wuhan 430030, China; ²Department of Geriatrics, Tongji Hospital, Tongji Medical College, Huazhong University of Science and Technology, Wuhan 430030, China

Aim: Neferine is an isoquinoline alkaloid isolated from seed embryos of *Nelumbo nucifera* (Gaertn), which has a variety of biological activities. In this study we examined the effects of neferine on Kv4.3 channels, a major contributor to the transient outward current (I_{to}) in rabbit heart, and on ex vivo electrophysiology of rabbit hearts.

Methods: Whole-cell Kv4.3 currents were recorded in HEK293 cells expressing human cardiac Kv4.3 channels using patch-clamp technique. Arterially perfused wedges of rabbit left ventricles (LV) were prepared, and transmembrane action potentials were simultaneously recorded from epicardial (Epi) and endocardial (Endo) sites with floating microelectrodes together with transmural electrocardiography (ECG).

Results: Neferine (0.1–100 $\mu\text{mol/L}$) dose-dependently and reversibly inhibited Kv4.3 currents (the IC_{50} value was 8.437 $\mu\text{mol/L}$, and the maximal inhibition at 100 $\mu\text{mol/L}$ was 44.12%). Neferine (10 $\mu\text{mol/L}$) caused a positive shift of the steady-state activation curve of Kv4.3 currents, and a negative shift of the steady-state inactivation curve. Furthermore, neferine (10 $\mu\text{mol/L}$) accelerated the inactivation but not the activation of Kv4.3 currents, and markedly slowed the recovery of Kv4.3 currents from inactivation. Neferine-induced blocking of Kv4.3 currents was frequency-dependent. In arterially perfused wedges of rabbit LV, neferine (1, 3, and 10 $\mu\text{mol/L}$) dose-dependently prolonged the QT intervals and action potential durations (APD) at both Epi and Endo sites, and caused dramatic increase of APD_{10} at Epi sites.

Conclusion: Neferine inhibits Kv4.3 channels likely by blocking the open state and inactivating state channels, which contributes to neferine-induced dramatic increase of APD_{10} at Epi sites of rabbit heart.

Keywords: neferine; Kv4.3; HEK293 cells; whole-cell patch-clamp; rabbit left ventricular wedge; action potential duration; electrocardiography

Acta Pharmacologica Sinica (2015) 36: 1451–1461; doi: 10.1038/aps.2015.83; published online 23 Nov 2015

Introduction

The activity of voltage-dependent K^+ (Kv) channels regulates the threshold, shape, duration, and frequency of action potentials in a wide variety of excitable cells^[1]. A transient outward current (I_{to})-mediated phase 1, which gives rise to a notched appearance of the action potential (AP), is now well established to be more prominent in the epicardium than in the endocardium of the ventricles of many species^[2]. The

presence of a prominent AP notch in the epicardium but not in the endocardium causes a transmural voltage gradient during ventricular activation that has been shown to underlie the J-wave and J-point elevation in the ECG^[3]. The presence of a prominent I_{to} -mediated notch also predisposes the ventricular epicardium to all-or-none repolarization under a variety of conditions, including ischemia^[4–6]. A loss of the AP dome (plateau) in the epicardium but not in the endocardium produces a voltage gradient during ventricular repolarization that is believed to underlie the elevation of the ST segment^[3].

Native I_{to} is encoded by A-type K^+ -channel genes, such as Kv1.4, Kv4.2, and Kv4.3^[7–9]. The participation of Kv4.3 has been convincingly demonstrated in rats^[8], rabbits^[7], dogs^[9] and

[#]These authors contributed equally to this work.

^{*}To whom correspondence should be addressed.

E-mail tangqiang_tjmu@hust.edu.cn

Received 2015-04-14 Accepted 2015-08-26

humans^[7]. Moreover, experimental studies of antisense oligodeoxynucleotides have also shown that Kv4.3 alone is a major component of I_{to} in the human and canine heart, whereas a combination of three cloned channels, Kv4.2, Kv4.3, and Kv1.4, is responsible for I_{to} in the rabbit atrium, which suggests that the physiological differences between the human and rabbit I_{to} may reflect the differential expression of subunit genes in K^+ channels^[7, 10].

Seed embryos from *Nelumbo nucifera* (Gaertn), also known as lotus, have been used in Chinese clinical practice as a traditional medicine for cardiovascular disease for over one thousand years. Neferine, which is an isoquinoline alkaloid ingredient in seed embryos from *Nelumbo nucifera* (Gaertn), has been demonstrated to have a wide range of biological activities, including preventing the onset of reentrant ventricular tachycardias after myocardial ischemia^[11-14]. However, reports of the effects of neferine on ion channels are sparse. Li *et al* first reported that neferine may inhibit the slow transmembrane Na^+ and/or L-type Ca^{2+} current in myocardium^[15]. Moreover, the direct effects of neferine on the human ether-a-go-go-related gene potassium current were recently reported by Gu *et al*^[16] and Dong *et al*^[17]. However, detailed studies of the interaction between neferine and I_{to} have not yet been published.

The present study aimed to determine the effects of neferine on Kv4.3 channels and the underlying potential effects of neferine on cardiac electrophysiology.

Materials and methods

Cell culture

HEK293 cells stably expressing the human cardiac Kv4.3 channel (a kind gift from Prof Gui-rong LI, University of Hong Kong) were maintained in Dulbecco's modified Eagle's medium (DMEM, HyClone) containing 10% (*v/v*) fetal bovine serum (FBS, Gibco) and 500 μ g/mL G418 (Sigma-Aldrich) at 37°C in 5% CO_2 -enriched air. The cells were seeded on sterile glass coverslips for 24–48 h before patch-clamp experiments.

Solutions and drugs

The extracellular bath solution contained the following (in mmol/L): 140 NaCl, 5 KCl, 1.8 $CaCl_2$, 1 $MgCl_2$, 0.33 NaH_2PO_4 , 10 HEPES, and 10 glucose (pH adjusted to 7.3 with NaOH). The pipette solution contained the following (in mmol/L): 20 KCl, 110 K-aspartate, 1 $MgCl_2$, 10 HEPES, 5 Mg-ATP, 5 EGTA, 5 Na_2 -phosphocreatine, and 0.1 GTP (pH adjusted to 7.2 with KOH). Neferine (purity \geq 97%, measured by HPLC) was provided by the Department of Pharmacology's Phytochemistry Laboratory of Tongji Medical College at the Huazhong University of Science and Technology (Wuhan, China)^[18]. It was dissolved in HCl and diluted with deionized water to obtain a 10 mmol/L stock solution (pH adjusted to 6.8 with NaOH). Quindine (Sigma) was dissolved in dimethyl sulfoxide (DMSO) to prepare a stock solution of 100 mmol/L. The stock solutions were stored at -20°C and diluted with the bath solution to obtain the desired concentration. The concentration of DMSO in the final dilution was less than 0.1%, and this concentration did not affect the Kv4.3 currents.

Patch-clamp recording

The Kv4.3 currents were recorded using the standard whole-cell patch-clamp technique. Cells on a cover slip were transferred to an open cell chamber mounted on the stage of an inverted microscope and superfused with bath solution at approximately 2 mL/min. Glass pipettes (1.5 mm diameter) were pulled with a two-stage microelectrode puller (PC-10, Narishige, Japan), and the resistance of the pipettes ranged from 2 to 4 M Ω when filled with the internal solution. The membrane currents were recorded with an EPC-10 amplifier and Pulse software (HEKA Elektronik, Lambrecht, Germany) at room temperature (21–23°C). The liquid junction potentials between the pipette and bath solutions were compensated before the pipette touched the cell. After giga-seal, the membrane was ruptured by gentle suction to establish the whole-cell configuration. The whole-cell capacitance and resistance were compensated, and the leak currents were subtracted. The current signal was filtered at 3 kHz and sampled at 10 kHz. Currents were recorded 5 min after achieving a whole-cell patch-clamp configuration.

Arterially perfused wedge of rabbit left ventricle

The methods used for surgical preparation, isolation, perfusion, and the recording of transmembrane activity from the arterially perfused rabbit left ventricle wedge preparation and the methods used to ensure the viability and electrical stability of the preparation were previously published and exactly followed^[19, 20]. Briefly, male New Zealand white rabbits weighing 2.5 to 3.0 kg were anticoagulated with 800 U/kg heparin (*iv*) and anesthetized with pentobarbital (50 mg/kg, *iv*). The rabbit's heart was rapidly excised and submerged in cold (4°C) cardioplegic solution containing 24 mmol/L K^+ buffered with 95% O_2 and 5% CO_2 . The left circumflex or anterior descending branch of the coronary artery was cannulated and perfused with the same cardioplegic solution. The unperfused areas of the left ventricle were removed and identified based on their reddish appearance. The preparation was then placed in a small heated tissue bath and arterially perfused with normal Tyrode's solution containing 4 mmol/L K^+ buffered with 95% O_2 and 5% CO_2 , maintained at 35.76 \pm 0.2°C; the perfusion pressure was maintained at 35 to 45 mmHg. The ventricular wedge was allowed to equilibrate in the tissue bath for 1 h prior to the electrical recordings. The preparation was paced at basic cycle lengths (BCLs) of 1000 ms.

A transmural pseudo-ECG was recorded with a pair of silver/silver chloride electrodes along the same vector as the transmembrane recordings. The transmembrane action potentials were recorded simultaneously from epicardial (Epi) and endocardial (Endo) sites with floating glass microelectrodes filled with 2.7 mol/L KCl. All amplified signals were digitized, stored on hard disk and analyzed using RM6240 (Chengdu, China). The action potential duration (APD) was measured at 90%, 50%, 20% and 10% of repolarization (APD₉₀, APD₅₀, APD₂₀ and APD₁₀).

Statistical analysis

The current was analyzed using Pulsefit (HEKA), and

nonlinear curve fitting was performed using SigmaPlot11.0 (SPSS Science, Chicago, IL, USA). Values are presented as the mean±SEM. Paired Student's *t*-tests were used to evaluate the significance of differences between two groups, whereas ANOVA was used to compare multiple groups. Values of $P < 0.05$ indicated significant differences.

Results

Effects of neferine on Kv4.3 channels

Kv4.3 currents were evoked by a single 500-ms depolarizing pulse to +50 mV from a holding potential of -80 mV. Superfusion with 10 μmol/L neferine significantly inhibited Kv4.3 currents (Figure 1A). The inhibitory effects of neferine on Kv4.3 currents were similar to those of quinidine: 10 μmol/L neferine reduced the peak outward currents by approximately 25.71%±1.23%, whereas 10 μmol/L quinidine reduced the peak outward currents by approximately 30.10%±4.01% ($n=7$,

$P > 0.05$) (Figure 1A and 1B). The concentration-dependent inhibition of Kv4.3 currents was investigated using 0.1–100 μmol/L neferine. The peak amplitudes of Kv4.3 currents at different concentrations of neferine were normalized to the fractional block percent relative to the control and then plotted against the concentration of neferine ($n=5-8$ for each concentration). The concentration-response curve was fitted to the Hill equation: $B(\%) = 100 / [1 + (IC_{50} / [D])^n]$, where $B(\%)$ is the fractional block percent change of the peak amplitude of Kv4.3 currents at a given neferine concentration $[D]$, IC_{50} is the concentration for 50% of maximum effect, and n is the Hill coefficient. The IC_{50} of neferine was 8.437 μmol/L for a Hill coefficient of 0.8605 (Figure 1C), and these parameters are similar to those of quinidine reported by Singarayar *et al*^[21].

Figure 2A shows the voltage-dependent blocking of Kv4.3 by neferine. Kv4.3 currents were evoked by 500-ms pulses ranging from -80 to +50 mV in steps of 10 mV every 5 s from

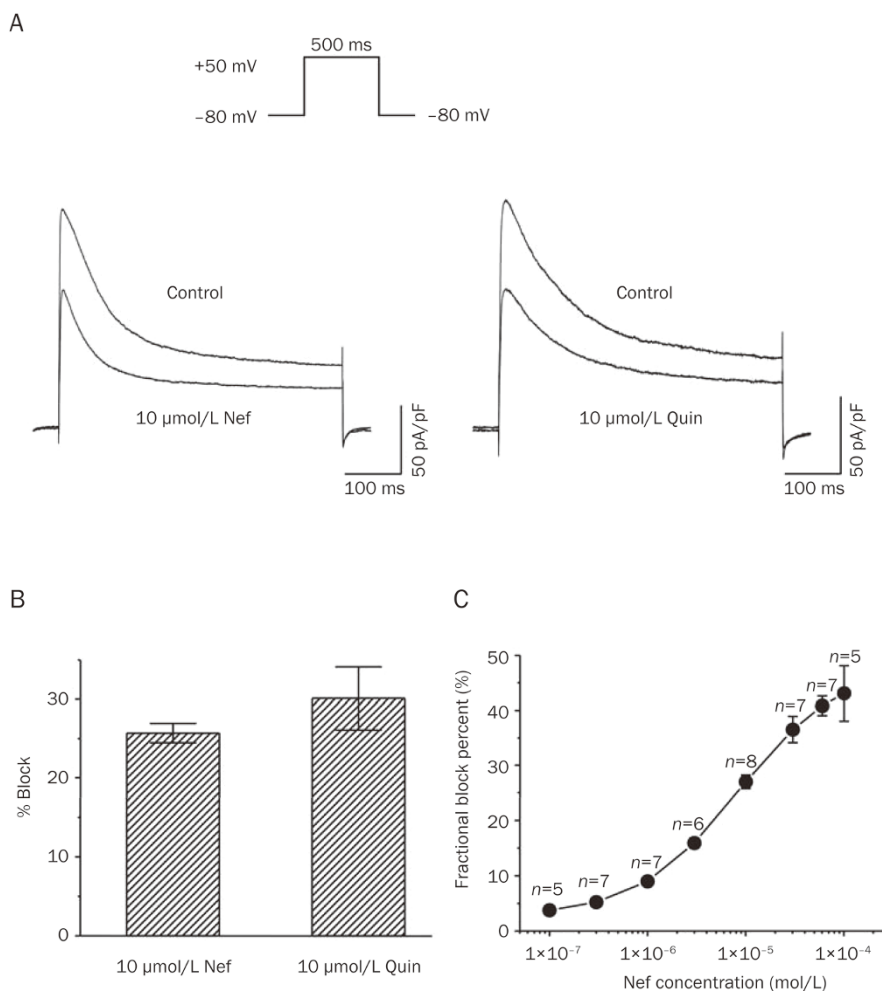


Figure 1. Effects of neferine and quinidine on Kv4.3 channels. (A) Representative traces showing Kv4.3 currents elicited by 500-ms pulses from -80 mV to +50 mV in the absence or presence of 10 μmol/L neferine (Nef) or 10 μmol/L quinidine (Quin). (B) Average percentage block of peak Kv4.3 currents in response to 10 μmol/L neferine and 10 μmol/L quinidine ($n=7$, $P > 0.05$). (C) The summarized data show the concentration-response curve; the plots indicate the percentage of blocked Kv4.3 currents at 0.1, 0.3, 1, 3, 10, 30, 60, and 100 μmol/L of neferine. The Hill equation was fitted to the normalized data ($n=5-8$ for each concentration). The data are expressed as the mean±SEM.

a holding potential of -80 mV. Neferine at 10 and 30 $\mu\text{mol/L}$ substantially suppressed the Kv4.3 currents, and this effect was reversed by washout. Figure 2B illustrates the current-voltage (I - V) relationships of Kv4.3 currents before and after the application of 3, 10, 30 $\mu\text{mol/L}$ neferine and washout ($n=6$, $P<0.05$).

The effects of 10 $\mu\text{mol/L}$ neferine on the steady-state activation of Kv4.3 channels were examined using double-pulse protocols. The amplitudes of tail currents were measured at -60

mV after the application of 8 ms depolarizing pulses stepping from -80 mV to $+100$ mV in 20 mV increments every 5 s from a holding potential of -80 mV. Figure 2C shows the summarized data for the activation in the absence and presence of 10 $\mu\text{mol/L}$ neferine. The steady-state activation curve was fitted to the Boltzmann equation: $I/I_{\text{max}}=a/[1+\exp[-(V-V_{1/2})/k]]$, where I_{max} represents the current measured at the most depolarized preconditioning pulse, V is the test potential, $V_{1/2}$ represents the point at which channels were half-activated, and k is the

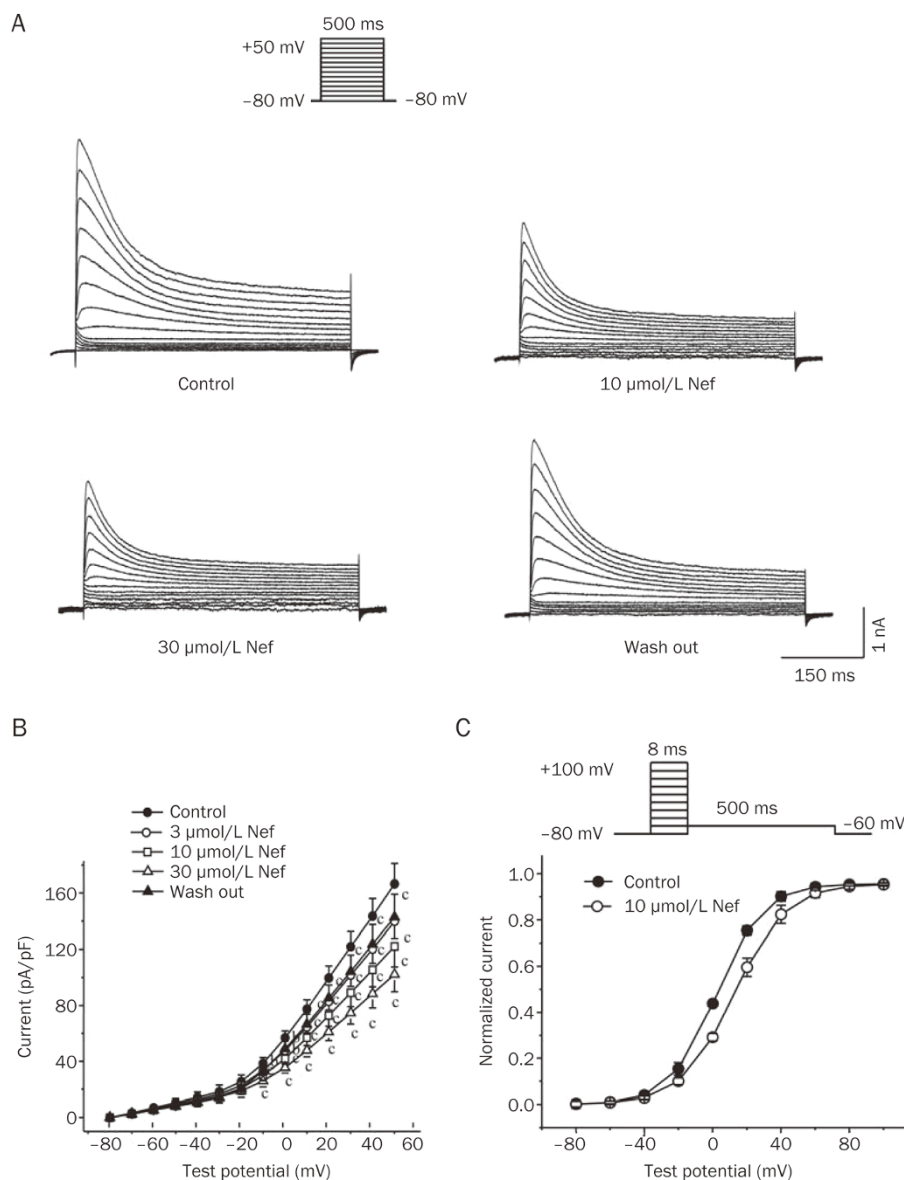


Figure 2. Concentration-dependent block of Kv4.3 channels by neferine. (A) The voltage-dependent Kv4.3 currents were recorded in a representative cell. The currents were evoked by 500-ms depolarizing pulses ranging from -80 to $+50$ mV in steps of 10 mV every 5 s from a holding potential of -80 mV. (B) Current-voltage (I - V) relationships of Kv4.3 currents before and after the application of 3, 10, 30 $\mu\text{mol/L}$ neferine and washout ($n=6$). (C) The steady-state activation of Kv4.3 currents was evoked using a double-pulse protocol: the membrane potential was held at -80 mV and then stepped from -80 mV to $+100$ mV for 8 ms in increments of 20 mV followed by a 500-ms pulse to -60 mV. The steady-state activation curves of Kv4.3 currents in the absence or presence of 10 $\mu\text{mol/L}$ neferine were fitted to the Boltzmann equation ($n=8$, $P<0.05$). The data are expressed as the mean \pm SEM. ^b $P<0.05$, ^c $P<0.01$ vs control.

slope factor. The steady-state activation curve was positively shifted by 10 $\mu\text{mol/L}$ neferine: the $V_{1/2}$ values of the control were 2.52 ± 0.76 mV, whereas those of the 10 $\mu\text{mol/L}$ neferine treatment were 15.07 ± 1.99 mV ($n=8$, $P < 0.05$); the slope factors were 13.62 ± 0.95 for the control and 16.23 ± 1.45 for 10 $\mu\text{mol/L}$ neferine ($n=8$, $P > 0.05$).

Effects of neferine on steady-state inactivation of Kv4.3 channels

The voltage dependence of the steady-state inactivation of Kv4.3 currents was determined using a conventional double-pulse protocol: holding the membrane potential at -80 mV and then stepping from -120 mV to $+50$ mV for 500 ms with increments of 10 mV followed by a 500-ms depolarizing pulse to $+50$ mV at 5 s intervals (Figure 3A). The Boltzmann equation was fitted to the steady-state inactivation curve: $(I-I_0)/$

$(I_{\text{max}}-I_0)=a/[1+\exp(V-V_{1/2})/k]$, where I_{max} represents the current measured at the most hyperpolarized preconditioning pulse, I_0 represents a non-inactivating current at the most depolarized preconditioning pulse, and $V_{1/2}$ represents the point at which channels were half-inactivated. The steady-state inactivation curve was negatively shifted by 10 $\mu\text{mol/L}$ neferine (Figure 3B): the $V_{1/2}$ value of the control was -30.18 ± 7.13 mV, whereas that of 10 $\mu\text{mol/L}$ neferine was -37.85 ± 7.92 mV ($n=5$, $P < 0.05$); the slope factor was 11.67 ± 2.33 for the control and 9.36 ± 0.93 for 10 $\mu\text{mol/L}$ neferine ($n=5$, $P > 0.05$).

Effects of neferine on the time constants of activation and inactivation

The time constants of activation (from the start of depolarizing pulses to the peak) and inactivation (from the peak to the end

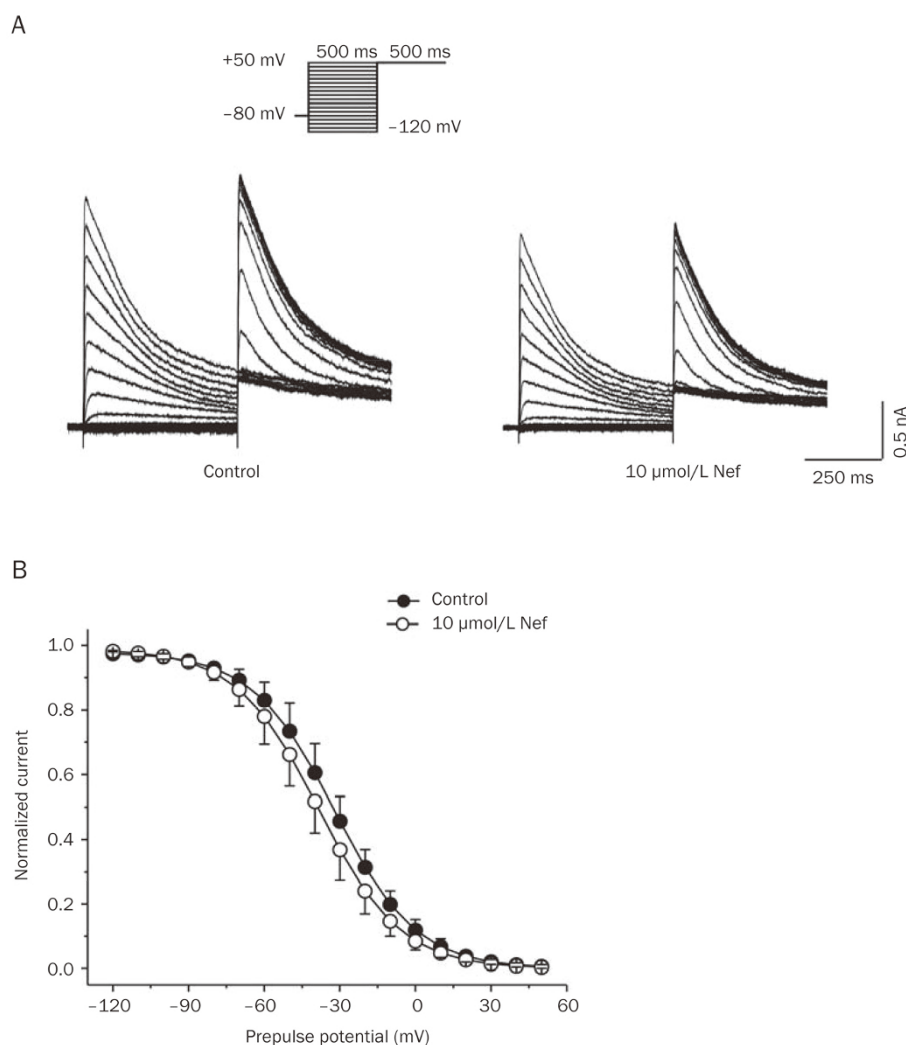


Figure 3. Effects of neferine on steady-state inactivation of Kv4.3 channels. (A) Representative traces show the steady-state inactivation of Kv4.3 currents, which were evoked using a two-pulse protocol. The membrane potential was held at -80 mV and then stepped from -120 to $+50$ mV in 500 ms in increments of 10 mV followed by a 500-ms depolarizing pulse to $+50$ mV in the absence or presence of 10 $\mu\text{mol/L}$ neferine. (B) Steady-state inactivation curves of Kv4.3 currents were fitted to the Boltzmann equation; the plots represent the normalized peak currents during the test pulse as a function of the conditioning potential ($n=5$, $P < 0.05$). The data are expressed as the mean \pm SEM.

of depolarizing pulses) of Kv4.3 currents fit a single-exponential function well. The activation time constants were not altered (Figure 4A, $n=7$, $P>0.05$), whereas 10 $\mu\text{mol/L}$ neferine decreased the inactivation time constants at test potential from +10 mV to +50 mV (the inactivation time constants were decreased from 102.52 ± 4.57 ms for control to 92.02 ± 3.85 ms at +50 mV) (Figure 4B, $n=7$, $P<0.05$).

Frequency-dependent effects of neferine on Kv4.3 currents

The frequency dependence of the effect of neferine was evaluated using 10 consecutive 200-ms depolarizing pulses to +50 mV from a holding potential of -80 mV at 0.5, 1 and 2 Hz (Figure 5A). The amplitude elicited by the second to tenth episode of the train was normalized to that elicited by the first episode and plotted against the given frequency (Figure 5B). The reduction in the first depolarizing pulse was considered to be the tonic block, and the reduction in subsequent pulses was considered to be frequency-dependent inhibition^[22]. The tonic blocks of 10 $\mu\text{mol/L}$ neferine were $24.79\%\pm 1.47\%$ at 0.5 Hz, $24.95\%\pm 1.25\%$ at 1 Hz and $24.63\%\pm 1.46\%$ at 2 Hz ($n=5$, $P>0.05$). Consistent with a previous observation^[1], significant decreases in the Kv4.3 current were observed at 1 and 2 Hz (compared with that of the first episode). The frequency-dependent inhibition of the Kv4.3 current by 10 $\mu\text{mol/L}$ neferine was observed at a frequency ≥ 1 Hz. The block of Kv4.3 current at the tenth stimulus of the train increased from $26.98\%\pm 1.61\%$ at 0.5 Hz to $28.96\%\pm 1.49\%$ at 1 Hz ($n=5$, $P<0.05$) and $33.08\%\pm 1.37\%$ at 2 Hz ($n=5$, $P<0.01$) (Figure 5C).

Effects of neferine on the time course of recovery from inactivation

The increase in blocking by neferine at faster rates suggests a time-dependent recovery after repolarization. The time course of recovery from inactivation was determined using a double-pulse protocol. The cells were depolarized to +50 mV for 500 ms (P1) from a holding potential of -80 mV, then returned to

the holding potential for a variable time interval between 50 and 5000 ms, followed by a second 500-ms pulse to +50 mV (P2) (Figure 6A). The peak amplitude of the second pulse (P2) was normalized to the corresponding first peak (P1) amplitude. The normalized data were plotted against the interpulse interval. The recovery curve fitted a single-exponential function well: $y=y_0+A_1[1-\exp(-t/\tau)]$, where τ represents the time course of the recovery from inactivation. A dose of 10 $\mu\text{mol/L}$ neferine significantly slowed the recovery from the inactivation of Kv4.3 current and increased the τ from 278.08 ± 30.52 ms to 331.40 ± 30.82 ms ($n=6$, $P<0.05$) (Figure 6B and 6C).

Effects of neferine on the transmembrane action potentials and QT intervals

Neferine elicited a concentration-dependent (1–10 $\mu\text{mol/L}$) lengthening of the action potential duration (APD) (Figure 7B): the APD₁₀ at Epi sites dramatically increased from 8.67 ± 2.28 ms of the control to 19.97 ± 4.51 ms, 27.96 ± 5.41 ms and 49.95 ± 6.57 ms at 1, 3 and 10 $\mu\text{mol/L}$ neferine, respectively ($n=8$, $P<0.05$). The APD₂₀ at Epi sites significantly increased from 58.01 ± 4.10 ms of the control to 65.98 ± 3.78 ms, 71.79 ± 8.47 ms and 104.69 ± 9.50 ms at 1, 3 and 10 $\mu\text{mol/L}$ neferine, respectively ($n=8$, $P<0.05$). A dose of 10 $\mu\text{mol/L}$ neferine slightly lengthened the APD₅₀ and APD₉₀ at Epi sites from 167.33 ± 7.59 ms of the control to 221.65 ± 15.41 ms and from 246.44 ± 15.58 ms of the control to 301.08 ± 13.06 ms, respectively ($n=8$, $P<0.05$). However, 1 and 3 $\mu\text{mol/L}$ neferine did not significantly affect the APD₅₀ and APD₉₀. Similar results were observed at Endo sites: 1 and 3 $\mu\text{mol/L}$ neferine did not significantly affect the APD at Endo sites. The relative prolongation of APD is shown in Figure 7C. The effects of neferine on the APD₁₀ at Epi sites were stronger than that at Endo sites. The APD₁₀ at Epi sites increased approximately $566.96\%\pm 103.64\%$, whereas the APD₁₀ at Endo sites increased only $117.98\%\pm 25.44\%$ in response to 10 $\mu\text{mol/L}$ neferine. The dispersion of APD₁₀ (the difference

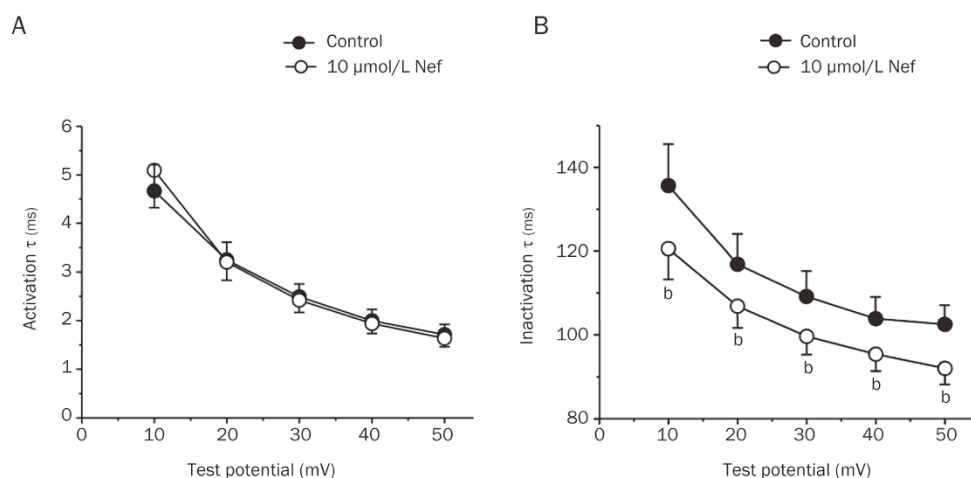


Figure 4. Effects of neferine on the time constants of activation and inactivation of Kv4.3 channels. Time constants (τ) of activation (A) and inactivation (B) at different voltages determined by fitting the mono-exponential functions. The data are expressed as the mean \pm SEM. $n=7$. ^b $P<0.05$ vs control.

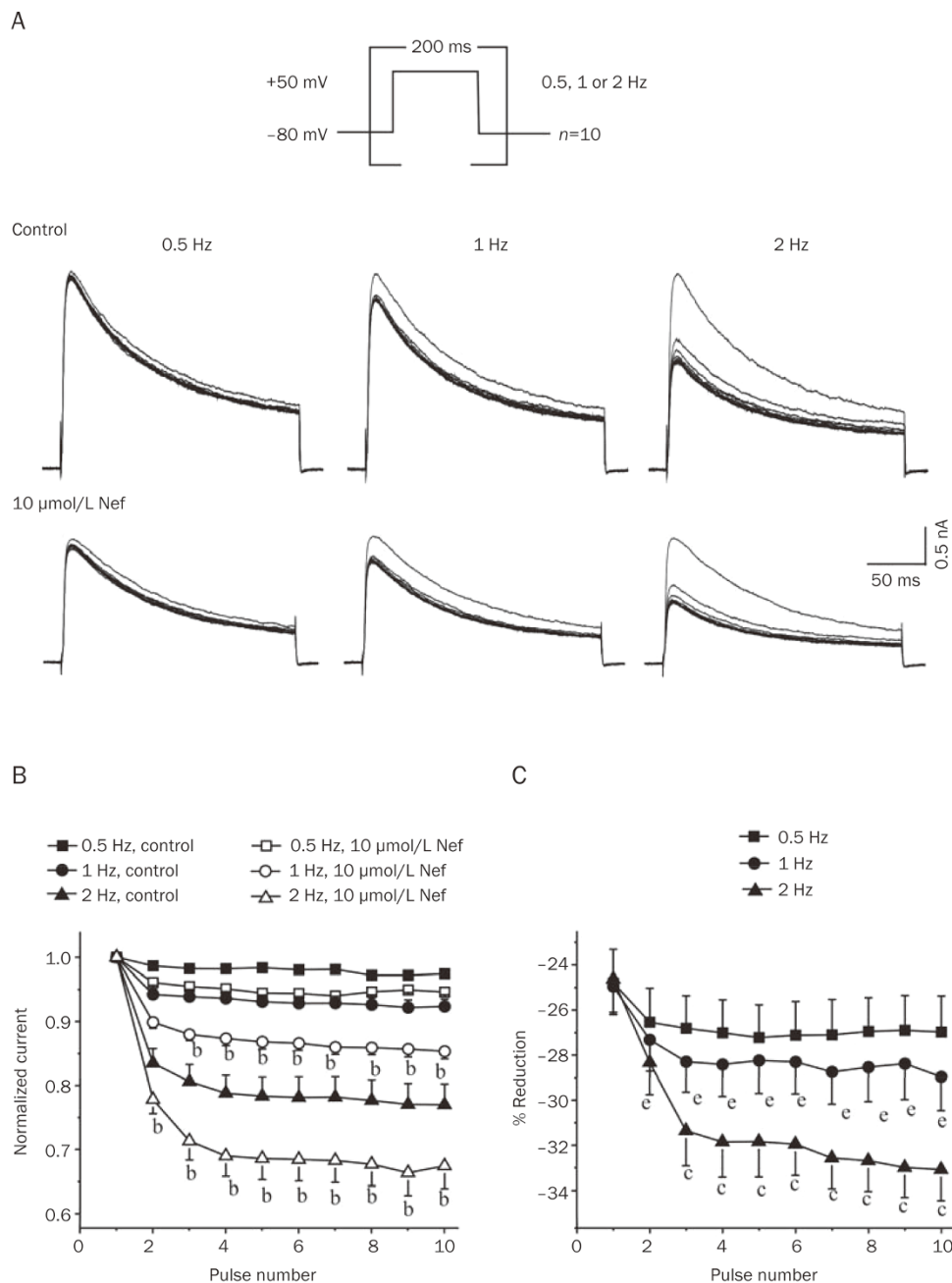


Figure 5. Frequency-dependent block of Kv4.3 channels by neferine. (A) Ten repetitive 200-ms depolarizing pulses of +50 mV from a holding potential of -80 mV were applied at three different frequencies, 0.5, 1 and 2 Hz, in the absence or presence of 10 μmol/L neferine. (B) The peak amplitudes of currents at each pulse were normalized to the peak amplitude of currents obtained at the first pulse (I_n/I_1) and then plotted against the pulse numbers. (C) Neferine (10 μmol/L) induced changes (%) in the current amplitude relative to the control [$(I_{Nef}-I_{cont})/I_{cont}$]. The data are expressed as the mean±SEM. $n=5$. ^b $P<0.05$, ^c $P<0.01$ vs control. ^e $P<0.05$ vs 0.5 Hz.

of APD₁₀ between Epi and Endo) decreased from 21.51±2.81 ms of the control to 13.37±3.40 ms at 10 μmol/L neferine ($n=8$, $P<0.05$).

Consistent with the effects on APD, neferine prolonged the QT intervals in a concentration-dependent manner (Figure 7D). Specifically, the QT intervals increased from 315.5±10.4 ms of the control to 318.9±11.1, 346.5±16.8 ms, and 424.3±19.3

ms at 1, 3 and 10 μmol/L neferine, respectively ($n=8$, $P<0.05$). The relative prolongation of the QT intervals is shown in Figure 7E.

Discussion

This study yielded the following novel findings: (1) Neferine potently and reversibly inhibits Kv4.3 currents in a concentra-

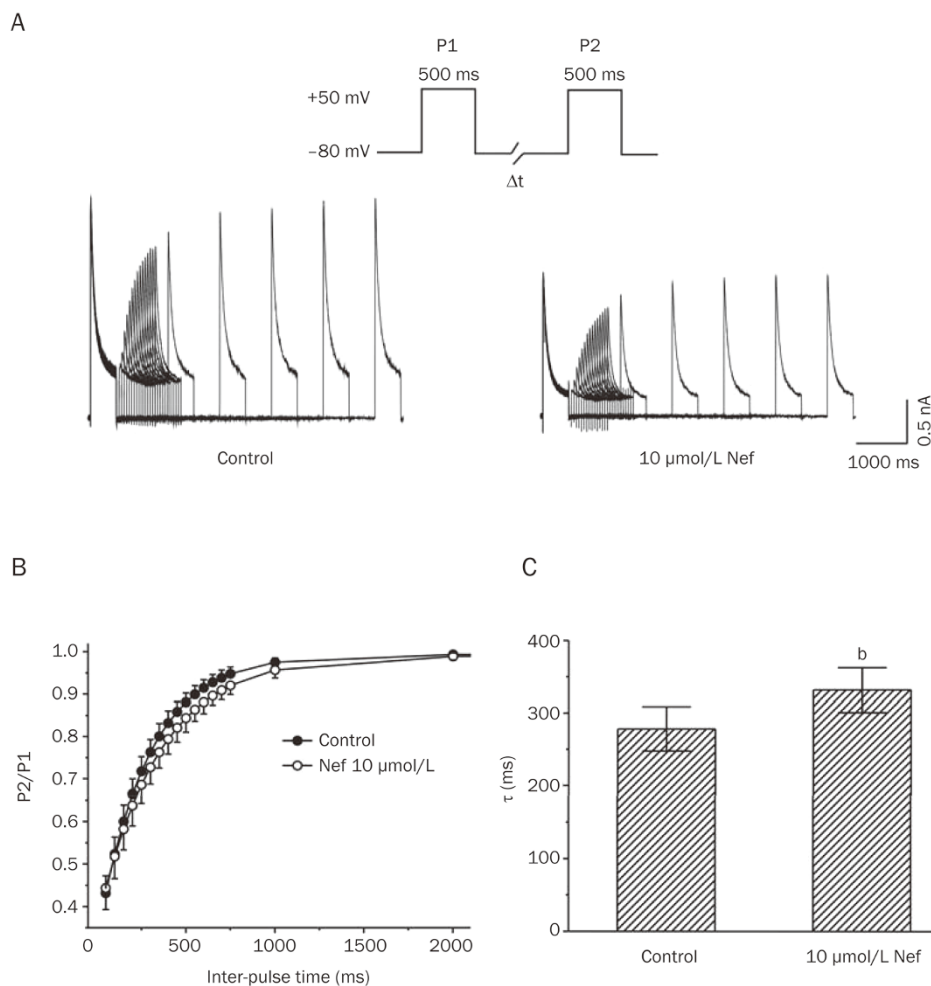


Figure 6. Effects of neferine on recovery from the inactivation of Kv4.3 channels. (A) Representative traces show the recovery of Kv4.3 channels from inactivation evoked by the double pulse protocol in the absence or presence of neferine. The cells were depolarized to +50 mV for 500 ms (P1) from a holding potential of -80 mV, then returned to the holding potential for a variable time interval between 50 and 5000 ms followed by a second 500-ms pulse to +50 mV (P2). (B) The time courses of recovery from inactivation in the absence or presence of 10 $\mu\text{mol/L}$ neferine. Summarized data are plotted as the relative amplitude of $I_{Kv4.3}$ (I_{P2}/I_{P1}) against the inter-pulse interval. The recovery curves fitted a single-exponential function well. (C) The data show the average recovery time constant (τ) in the absence or presence of 10 $\mu\text{mol/L}$ neferine. The data are expressed as the mean \pm SEM. $n=6$. ^b $P<0.05$ vs control.

tion-dependent and frequency-dependent manner; (2) neferine significantly shifts the steady-state activation curve of Kv4.3 currents in a positive direction while shifting the steady-state inactivation curve in a negative direction; (3) neferine accelerates the inactivation and decelerates the recovery from the inactivation of Kv4.3 currents; (4) neferine significantly prolongs the QT intervals and APD at Epi and Endo sites in rabbit left ventricle wedges, especially the APD₁₀, which was dramatically extended at Epi sites. The present work demonstrates that neferine is a potent direct blocker of I_{to} and may contribute to the ability of neferine to dramatically increase the APD₁₀ at Epi sites.

Kv4.3 channels, which are members of the shal-type rapidly activating and inactivating Kv channels, encode the transient outward potassium currents (I_{to}) in the heart^[9], which are

responsible for phase 1 of the cardiac action potential^[23]. I_{to} is altered in many heart diseases and is consequently a target of many drugs^[24, 25].

The present study indicated that neferine potently inhibited Kv4.3 currents in a concentration-dependent manner, with a half-maximal inhibition (IC_{50}) of 8.437 $\mu\text{mol/L}$ (Figure 1C). Recent pharmacokinetic and tissue distribution measurements in rats showed that the concentration of neferine in the heart was 11.1 ± 6.8 $\mu\text{mol/L}$ 30 min after a tail vein injection of 25 mg/kg neferine^[26]. Therefore, the concentration of neferine needed to block Kv4.3 channels can be achieved.

In the present study, neferine treatment resulted in the frequency-dependent inhibition of Kv4.3 currents and a subsequent slow recovery from this inactivation. Frequency-dependent blocking is the most common characteristic of

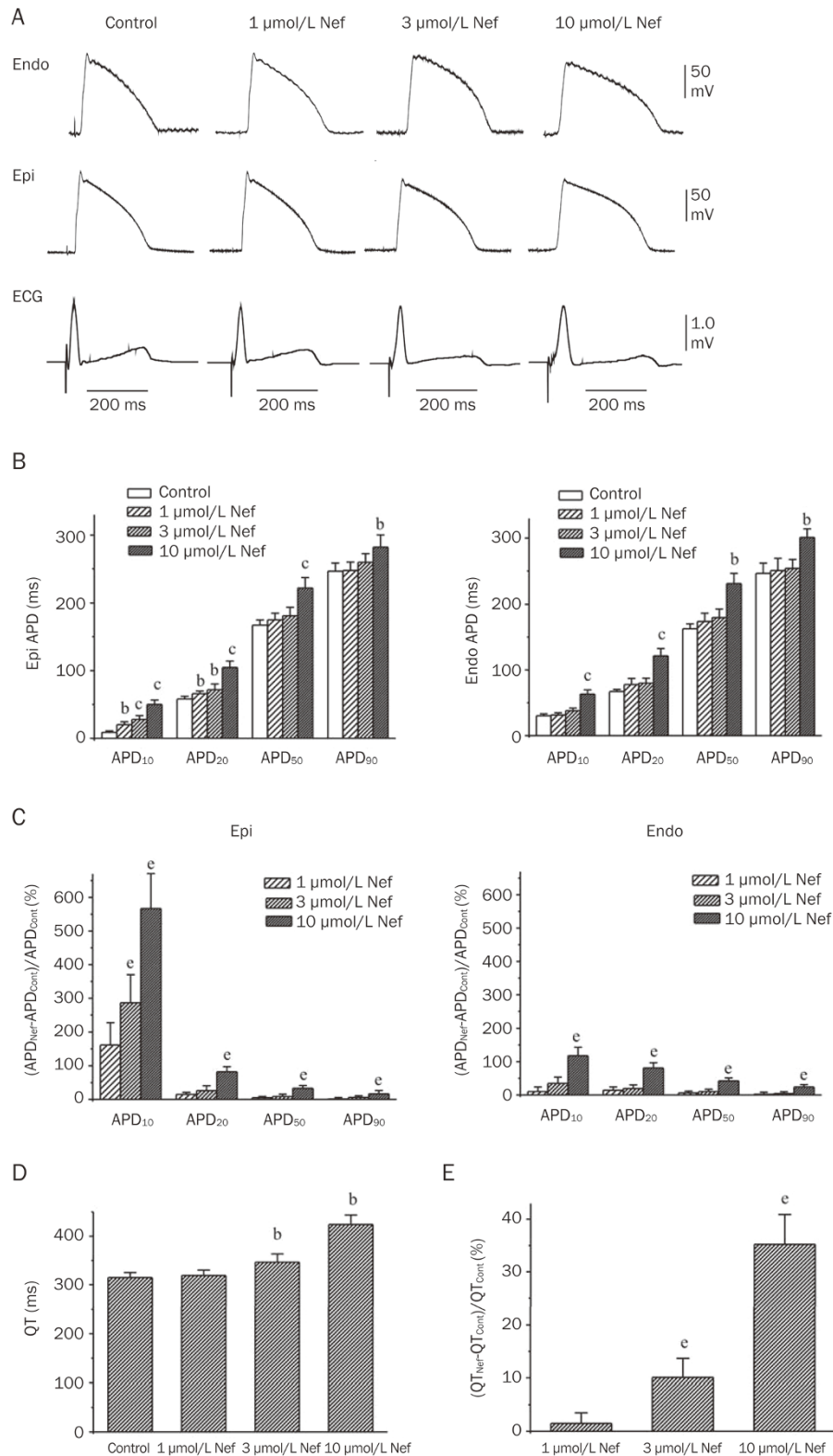


Figure 7. Effects of neferine on the transmembrane action potentials and ECG. (A) Original trace showing APs simultaneously recorded at endocardial (Endo) and epicardial (Epi) sites, together with a transmural ECG recorded in a rabbit left ventricular wedge. (B) Summary data show the effects of neferine on APD at Endo and Epi sites. (C) Relative prolongation of APD at Endo and Epi sites with 1, 3 and 10 $\mu\text{mol/L}$ neferine. (D) Summary data show the effects of neferine on QT intervals. (E) Relative prolongation of QT intervals with 1, 3 and 10 $\mu\text{mol/L}$ neferine. The data are expressed as the mean \pm SEM. $n=8$. ^b $P<0.05$, ^c $P<0.01$ vs control. ^e $P<0.05$ vs 1 $\mu\text{mol/L}$ neferine.

open-channel blockade in many drugs, such as quinidine^[21, 27], flecainide^[27], nicardipine^[1]. Accelerated blocking suggests that depolarization enhances the drug's effect on the channel and that time-dependent recovery occurs after inactivation. The characteristics of the frequency-dependent blocking suggest that neferine is another open-channel blocker of Kv4.3 channels.

Neferine accelerated the inactivation of Kv4.3 channels and significantly negatively shifted the steady state inactivation curve, which is similar to the quinidine-induced blocking of Kv4.3 currents^[21]. However, the ability of open channel blockers to shift the inactivation curve has been debated. Wang *et al*^[27] suggested that the accelerated inactivation without a shift in the voltage dependence of inactivation in the quinidine-induced blocking of the Kv4.3 current is consistent with open-channel blockade, whereas a negative shift in the voltage dependence of inactivation in the flecainide-induced blocking of Kv4.3 current is consistent with a preferential inactivated-channel blockade. However, Singarayar *et al* reported a negative shift in the voltage dependence of the quinidine-induced blocking of Kv4.3 currents^[21] (the contradicting effects of quinidine on the Kv4.3 current inactivation curve may not be due to the differences in the cells used in these studies). Other agents that act as open-channel blockers of Kv4.3, such as dapoxetine^[28] and duloxetine^[29], also negatively shifted the voltage dependence of inactivation of the Kv4.3 current. These apparently open channel blockers can also bind to the inactivated state of channels. A similar effect on other channels has also been observed for other open channel blockers such as pergolide that negatively shifted the voltage dependence of inactivation of Kv1.5 currents^[30], and BAPTA-AM and ketaserin, which negatively shifted the voltage dependence of the inactivation of hERG currents^[31, 32]. This effect may be attributed to the following: Kv4.3 currents, like $I_{Kv1.5}$ ^[30] and I_{hERG} ^[32], are characterized by a current window in which the steady-state activation curve and inactivation curve overlap, which allows neferine to simultaneously bind the open state and the inactivated state of channels, like other open channel blockers. Unlike the quinidine-induced blocking of Kv4.3 currents, which did not shift the steady state activation curve^[21], neferine shifted the steady state activation curve of Kv4.3 currents in a depolarizing direction. A positive shift in the steady state activation curve of Kv4.3 currents suggested that the reactivation of the channel was difficult upon the binding of neferine.

I_{to} -mediated phase 1, which gives rise to a notched appearance of the action potential (AP), is more prominent in the epicardium than the endocardium of the ventricles of many species^[2]. Kv4.2, Kv4.3, and Kv1.4 are the major constituents of native cardiac I_{to} in the rabbit atrium^[7]. The ability of neferine to block the Kv4.3 current might assist the observed lengthening of cardiac APD₁₀, APD₂₀ and QT intervals. Because of the differences in the distribution of I_{to} between the epicardium and endocardium of the ventricles, neferine dramatically increased APD₁₀ at Epi sites. Neferine preferentially prolongs the initial repolarization and the subsequent plateau phases, which is consistent with the participation of I_{to} in early phases

of repolarization. The blockade of I_{to} may also explain the neferine-induced decrease of the dispersion of APD₁₀ because neferine may shrink the voltage gradients between epicardial and endocardial sites. These effects may prevent phase 2 reentry and contribute to prevent the onset of reentrant ventricular tachycardia after myocardial ischemia. However, the excessive blocking of I_{to} could also be proarrhythmic. Obviously, the anti-arrhythmic consequences of neferine action on I_{to} await further study.

In conclusion, neferine is a potent inhibitor of Kv4.3 channels that likely functions by blocking the open state and inactivating the state of channels. This action may contribute to the ability of neferine to dramatically increase the APD₁₀ at Epi sites.

Acknowledgments

We thank Dr Gui-rong LI (University of Hong Kong) for providing the HEK293 cells that stably expressed Kv4.3 potassium channels.

Author contribution

Qiang TANG, Ji-zhou XIANG and Cun-tai ZHANG designed the study; Chen WANG, Yu-fang CHEN, Xiao-qing QUAN, Huan WANG, Rui ZHANG, Jun-hua XIAO and Jia-ling WANG performed the experiments; Chen WANG and Yu-fang CHEN analyzed the data; Xiao-qing QUAN, Huan WANG, Rui ZHANG, Jun-hua XIAO and Jia-ling WANG contributed the reagents and materials; Chen WANG, Yu-fang CHEN, Ji-zhou XIANG and Qiang TANG wrote the paper.

References

- 1 Hatano N, Ohya S, Muraki K, Giles W, Imaizumi Y. Dihydropyridine Ca²⁺ channel antagonists and agonists block Kv4.2, Kv4.3 and Kv1.4 K⁺ channels expressed in hek293 cells. *Br J Pharmacol* 2003; 139: 533–44.
- 2 Yan GX, Antzelevitch C. Cellular basis for the brugada syndrome and other mechanisms of arrhythmogenesis associated with st-segment elevation. *Circulation* 1999; 100: 1660–6.
- 3 Yan GX, Antzelevitch C. Cellular basis for the electrocardiographic J wave. *Circulation* 1996; 93: 372–9.
- 4 Di Diego JM, Antzelevitch C. Pinacidil-induced electrical heterogeneity and extrasystolic activity in canine ventricular tissues. Does activation of atp-regulated potassium current promote phase 2 reentry? *Circulation* 1993; 88: 1177–89.
- 5 Krishnan SC, Antzelevitch C. Flecainide-induced arrhythmia in canine ventricular epicardium. Phase 2 reentry? *Circulation* 1993; 87: 562–72.
- 6 Lukas A, Antzelevitch C. Phase 2 reentry as a mechanism of initiation of circus movement reentry in canine epicardium exposed to simulated ischemia. *Cardiovasc Res* 1996; 32: 593–603.
- 7 Wang Z, Feng J, Shi H, Pond A, Nerbonne JM, Nattel S. Potential molecular basis of different physiological properties of the transient outward K⁺ current in rabbit and human atrial myocytes. *Circ Res* 1999; 84: 551–61.
- 8 Fiset C, Clark RB, Shimon Y, Giles WR. Shal-type channels contribute to the Ca²⁺-independent transient outward K⁺ current in rat ventricle. *J Physiol* 1997; 500: 51–64.
- 9 Dixon JE, Shi W, Wang HS, McDonald C, Yu H, Wymore RS, *et al*. Role

- of the kv4.3 K⁺ channel in ventricular muscle. A molecular correlate for the transient outward current. *Circ Res* 1996; 79: 659–68.
- 10 Kong W, Po S, Yamagishi T, Ashen MD, Stetten G, Tomaselli GF. Isolation and characterization of the human gene encoding I_{to}: Further diversity by alternative mrna splicing. *Am J Physiol* 1998; 275: H1963–70.
 - 11 Huang HL, Rao MR. Effects of neferine and its combination with taurine on platelet aggregation and experimental thrombosis in rats. *Acta Pharm Sin* 1995; 30: 486–90.
 - 12 Guo Z. Electrophysiological effects of neferine against ischemic ventricular tachyarrhythmias. *Zhonghua Xin Xue Guan Bing Za Zhi* 1992; 20: 119–122, 134.
 - 13 Pan Y, Cai B, Wang K, Wang S, Zhou S, Yu X, et al. Neferine enhances insulin sensitivity in insulin resistant rats. *J Ethnopharmacol* 2009; 124: 98–102.
 - 14 Yoon JS, Kim HM, Yadunandam AK, Kim NH, Jung HA, Choi JS, et al. Neferine isolated from nelumbo nucifera enhances anti-cancer activities in hep3b cells: Molecular mechanisms of cell cycle arrest, er stress induced apoptosis and anti-angiogenic response. *Phytomedicine* 2013; 20: 1013–22.
 - 15 Li GR, Li XG, Lu FH. Effects of neferine on transmembrane potential in rabbit sinoatrial nodes and clusters of cultured myocardial cells from neonatal rats. *Acta Pharmacol Sin* 1989; 10: 328–31.
 - 16 Gu DF, Li XL, Qi ZP, Shi SS, Hu MQ, Liu DM, et al. Blockade of herg K⁺ channel by isoquinoline alkaloid neferine in the stable transfected hek293 cells. *Naunyn-Schmiedeberg's Arch Pharmacol* 2009; 380: 143–51.
 - 17 Dong ZX, Zhao X, Gu DF, Shi YQ, Zhang J, Hu XX, et al. Comparative effects of liensinine and neferine on the human ether-a-go-go-related gene potassium channel and pharmacological activity analysis. *Cell Physiol Biochem* 2012; 29: 431–42.
 - 18 Huang Y, Zhao L, Bai Y, Liu P, Wang J, Xiang J. Simultaneous determination of liensinine, isoliensinine and neferine from seed embryo of nelumbo nucifera gaertn. In rat plasma by a rapid hplc method and its application to a pharmacokinetic study. *Arzneimittelforschung* 2011; 61: 347–52.
 - 19 Liu T, Brown BS, Wu Y, Antzelevitch C, Kowey PR, Yan GX. Blinded validation of the isolated arterially perfused rabbit ventricular wedge in preclinical assessment of drug-induced proarrhythmias. *Heart Rhythm* 2006; 3: 948–56.
 - 20 Yan GX, Shimizu W, Antzelevitch C. Characteristics and distribution of m cells in arterially perfused canine left ventricular wedge preparations. *Circulation* 1998; 98: 1921–7.
 - 21 Singarayay S, Bursill J, Wyse K, Bauskin A, Wu W, Vandenberg J, et al. Extracellular acidosis modulates drug block of Kv4.3 currents by flecainide and quinidine. *J Cardiovasc Electrophysiol* 2003; 14: 641–50.
 - 22 Wang H, Shi H, Zhang L, Pourrier M, Yang B, Nattel S, et al. Nicotine is a potent blocker of the cardiac a-type K⁺ channels. Effects on cloned Kv4.3 channels and native transient outward current. *Circulation* 2000; 102: 1165–71.
 - 23 Sah R, Ramirez RJ, Oudit GY, Gidrewicz D, Trivieri MG, Zobel C, et al. Regulation of cardiac excitation-contraction coupling by action potential repolarization: Role of the transient outward potassium current I_{to}. *J Physiol* 2003; 546: 5–18.
 - 24 Fischer F, Vonderlin N, Zitron E, Seyler C, Scherer D, Becker R, et al. Inhibition of cardiac Kv1.5 and Kv4.3 potassium channels by the class Ia anti-arrhythmic ajmaline: Mode of action. *Naunyn Schmiedebergs Arch Pharmacol* 2013; 386: 991–9.
 - 25 Delpon E, Cordeiro JM, Nunez L, Thomsen PE, Guerchicoff A, Pollevick GD, et al. Functional effects of kcne3 mutation and its role in the development of brugada syndrome. *Circ Arrhythm Electrophysiol* 2008; 1: 209–18.
 - 26 Lee HJ, Sung KW, Hahn SJ. Effects of haloperidol on kv4.3 potassium channels. *Eur J Pharmacol* 2014; 740: 1–8.
 - 27 Wang Z, Fermini B, Nattel S. Effects of flecainide, quinidine, and 4-aminopyridine on transient outward and ultrarapid delayed rectifier currents in human atrial myocytes. *J Pharmacol Exp Ther* 1995; 272: 184–96.
 - 28 Jeong I, Kim SW, Yoon SH, Hahn SJ. Block of cloned kv4.3 potassium channels by dapoxetine. *Neuropharmacology* 2012; 62: 2261–6.
 - 29 Choi JS, Hahn SJ. Duloxetine blocks cloned kv4.3 potassium channels. *Brain Res* 2012; 1466: 15–23.
 - 30 Jeong I, Choi BH, Hahn SJ. Pergolide block of the cloned kv1.5 potassium channels. *Naunyn-Schmiedeberg's Arch Pharmacol* 2013; 386: 125–33.
 - 31 Tang Q, Li ZQ, Li W, Guo J, Sun HY, Zhang XH, et al. The 5-HT2 antagonist ketanserin is an open channel blocker of human cardiac ether-a-go-go-related gene (herg) potassium channels. *Br J Pharmacol* 2008; 155: 365–73.
 - 32 Tang Q, Jin MW, Xiang JZ, Dong MQ, Sun HY, Lau CP, et al. The membrane permeable calcium chelator bapta-am directly blocks human ether a-go-go-related gene potassium channels stably expressed in HEK293 cells. *Biochem Pharmacol* 2007; 74: 1596–607.